Communication

Theory of Chiral Induced Spin Selectivity

Per Hedegard, and Sakse Dalum

Nano Lett., **Just Accepted Manuscript** • DOI: 10.1021/acs.nanolett.9b01707 • Publication Date (Web): 02 Jul 2019

Theory of Chiral Induced Spin Selectivity

Sakse Dalum[†,‡] and Per Hedegård[*,†]

†Niels Bohr Institute, University of Copenhagen, DK-2100 Copenhagen, Denmark

‡Sino-Danish Center for Education and Research (SDC), Eastern Yanqihu Campus, University of Chinese Academy of Sciences, Huaibeizhen, Huairou Qu, 101408 Beijing, China

E-mail: hedegard@nbi.ku.dk

Abstract

A general theory of the Chiral Induced Spin Selectivity (CISS) effect is presented. It is based on the fact that the spin-orbit (SO) coupling is small—a few meV—for the light atoms which make up typical chiral molecules in experiments. We present a theorem based on the Onsager reciprocal principle which states that the CISS effect *vanishes* when thermally averaging over all electron states. This zero-result is avoided by the very non-thermal character of the incoming optically generated electrons in experimental realizations. Despite the small SO-coupling, the presence of accidental degeneracies in the molecular spectrum yields a sizable spin polarization.

The CISS effect in the presence of magnetic leads is special. We prove that in a situation with one magnetic lead, the other lead will become magnetized. This results from the interplay between the spin-orbit coupling in the chiral molecule and the magnetized lead. Numerical calculations for realistic chiral molecules confirm the theory.

Keywords

Chiral Induced Spin Selectivity, spin polarization, spintronics, molecular electronics, electron transport

Introduction

The ability of chiral molecules to spin polarize electrons passing through is a truly remarkable fact. The effect is named CISS (Chiral Induced Spin Selectivity) and was initially reported in 1999 by Naaman and collaborators.[1] Since then, a number of additional experimental[2–17] and theoretical[18–35] studies have been conducted. However, a theoretical consensus has not yet emerged.

Intuitively, the CISS effect seems plausible from a semiclassical point of view. A prototypical chiral molecule is DNA which forms a helix. A helix is a coil, and a current carrying coil is the favorite source of magnetic fields in the macroscopic world. Further, it is commonly known that a magnetic field can polarize electrons, including the electrons that constitute the current. This macroscopic picture, however, breaks down at a microscopic level. First, the currents in the actual experiments is so small, that the time between subsequent electrons is large. Thus, only one electron is moving through a given molecule at a time. Second, if a magnetic field is present, the primary effect is to precess the direction of the spin of an electron. This alone leads to no polarization. For polarization to occur, spin relaxation processes must take place. Hence, any theory which involves a magnetic field has to explain the nature of spin relaxation processes.

At the microscopic level, we do know of a source of magnetic fields felt by electrons: the spin-orbit coupling. The physical picture is that from the point of view of an electron orbiting a nucleus, the nuclear charge is seen as a current going around the electron itself. This subjects the electron to a magnetic field. Since the effect is ultimately relativistic—i.e., the magnetic field is proportional to v/c^2E, where v is the velocity of the orbiting

electron and E is the electric field experienced by the electron—the magnetic field is quite small. Inside a light atom, the electric field $E \approx 1$ V/Å and the velocity $v \approx 1$ Å/fs resulting in a magnetic field $B \approx 10$ mT. For p-electrons in carbon, the magnitude of the resulting Zeeman energy is known from atomic physics to be ~ 6 meV, corresponding to a temperature of a few tens of kelvin. Magnetic fields resulting from electric fields other than the nuclear fields inside atoms can be ignored in this context, since they tend to be much weaker, and the velocities of electrons moving between atoms are also much lower. Still, the magnetic field of the atomic spin-orbit coupling is so small that a cumulative effect is necessary. This fact has been pointed out by Varela et al.[28]

The cumulative effect results from the fact that when an electron is passing through a molecule, it visits many different atoms. In each such visit, it will orbit the nucleus. Since the direction of the spin-orbit magnetic field depends on the orientation of the orbit, it is important that the orientations of the orbits visited by the electron are biased toward a specific direction. If this is not the case, the magnetic fields will cancel. We shall see that precisely in chiral molecules, such a preferred direction emerges when an electron moves through the molecule.

In this paper we first present two main results which are important for understanding the CISS effect. The results are based on the observation above that the spin-orbit (SO) coupling in light atoms is very weak. This allows for a perturbative approach.

To first order, the total spin is conserved for electrons being in contact with all kinds of molecules. So, if electrons moving through a molecule become polarized, the backscattered electrons will polarize in the opposite direction. Hence, there is no real spin relaxation taking place, in keeping with the general theory of spin relaxation, which is based on a second order calculation in the SO-coupling.

The second, and dramatic result, is that *if* 1) the incoming electrons are in equilibrium in the sense that all electron states with the same energy are equally probable, 2) there are only two leads (denoted left and right), *and* 3) the leads are non-magnetic, *then* there is *no*

polarization of the transmitted electrons.

These results are general in the sense that they will survive if temperature effects resulting from coupling to thermal vibrations in the system are included. The importance of the second requirement has already been anticipated by Matityahu et al.[27] who have shown that if so-called virtual Büttiker-Landauer leads are added to the theoretical setup, a much stronger spin polarization emerges.

The consequence of these theoretical findings is that one should seek the explanation of the CISS effect in features of the experimental setup which breaks with the premises of the theorems.

We identify three such breaks in current experiments: not all electrons with the same energy are equally probable, a preponderance of degeneracies in the electronic spectrum of the chiral molecules, and/or one of the leads is magnetic.

The recent experiments by Kumar et al.[11] involve induced dipole moments in electronically isolated molecules. If a chiral molecule is suddenly exposed to an electrical field, a temporary electrical current will be induced which builds up an electrical dipole moment in the molecule. Experimentally, this results in a transient magnetic moment of the molecule. This class of experiments is not covered by the theory presented here. The general perturbative approach, however, should also be possible in this latest generation of experiments.

Theory

We first consider a physical situation, where two metallic leads are connected by a single molecule, conventionally denoted *left* and *right*. This is the standard setup in current theories of molecular electronics and spintronics. The starting point is an electron prepared in a localized state in the left lead. For some time, a current will run through the molecule while the electron is either passing through to the right lead or is backscattered into the left. The associated particle current into the right lead is denoted $\langle \dot{R} \rangle$. Since electrons carry spin,

there is also an associated spin current. The rate of change of spin along a direction $\vec{n}$ is denoted $\langle S_{R\vec{n}} \rangle$. These two currents can be calculated theoretically, the mathematical details of which can be found in the supporting material.

To describe the process, we employ the so-called NEGF (Non-Equilibrium Green Function) technique. This involves an initial state described by a density matrix, ρ, and a physical quantity for which an average is calculated. The density matrix is of the form

$$\rho = \rho_e \otimes \rho_s, \quad \rho_e = \sum_i p_i |\phi_i\rangle\langle\phi_i|, \quad \rho_s = \frac{1}{2}(1 + \vec{\sigma} \cdot \vec{a}_{\text{in}}), \tag{1}$$

where ρ_e accounts for the knowledge of which orbitals the electron occupies initially, and ρ_s describes the initial knowledge about the spin state of the electron. The initial spin polarization of the state is given by the vector $\vec{a}_{\text{in}}$.

The physical quantities we are interested in are the particle and spin currents. The result for the currents into the right lead are

$$\langle \dot{R} \rangle = \int \text{Tr}[\gamma_L G_M^\dagger \Gamma_R G_M] \frac{dE}{2\pi}, \tag{2}$$

$$\langle S_{R\vec{n}} \rangle = \int \text{Tr}[\gamma_L G_M^\dagger \Gamma_R \, \vec{\sigma} \cdot \vec{n} \, G_M] \frac{dE}{2\pi}. \tag{3}$$

Here, γ_L and Γ_R are operators describing how the electron enters and exits the molecule, and the operator

$$G_M = \frac{1}{E - H_M + i\Gamma_L/2 + i\Gamma_R/2}, \tag{4}$$

describes its propagation through the molecule. Note that Γ_L and Γ_R are, in general, energy-dependent quantities.

Our focus in this paper is the spin of the electrons, in particular how the spin-orbit coupling of the atoms in the central molecule affects transmission. The spin orbit coupling

is part of the molecular Hamiltonian, H_M. It is given by

$$H_{SO} = \sum_i \lambda_i \vec{L}_i \cdot \vec{\sigma} = \vec{\Lambda} \cdot \vec{\sigma}. \tag{5}$$

Here $\vec{L}_i$ is the angular momentum operator of an electron on an atom labelled i. The strength of the coupling is given by the parameter λ_i. For the light atoms we consider, this energy is small; only a few meV for typical atoms involved (like C, N and O).

As discussed in the introduction, the SO interaction is a small perturbation. The NEGF expressions can, in a straightforward manner, be expanded to lowest order in the SO-coupling. The polarization of the electron emerging in the right lead is calculated using this expansion to be:

$$P_n = \frac{\langle S_{R\vec{n}} \rangle}{\langle \dot{R} \rangle} = \vec{a}_{out} \cdot \vec{n}, \quad \text{where,} \quad \vec{a}_{out} = \frac{\vec{a}_{\text{in}} + \vec{D} + \vec{C} \times \vec{a}_{\text{in}}}{1 + \vec{a}_{\text{in}} \cdot \vec{D}}. \tag{6}$$

Here, *two* vectors associated with the molecule emerge: $\vec{D}$ and $\vec{C}$. They are given by the real and imaginary parts of an auxiliary complex vector, $\vec{A}$:

$$\vec{D} = 2\,\mathrm{Re}[\vec{A}], \quad \vec{C} = 2\,\mathrm{Im}[\vec{A}], \quad \vec{A} = \frac{\mathrm{Tr}[\gamma_L G_M^{0\dagger} \vec{\Lambda} G_M^{0\dagger} \Gamma_R G_M^0]}{\mathrm{Tr}[\gamma_L G_M^{0\dagger} \Gamma_R G_M^0]}, \tag{7}$$

where G_M^0 is the Green's function of the molecule *without* SO-coupling. Note that both vectors are linear in $\vec{\Lambda}$ and thus the SO-coupling.

Since the vector operator $\vec{\Lambda}$ is an angular momentum and hence an axial vector, we know that $\vec{D}$ and $\vec{C}$ are axial vectors. When seen in a mirror, axial vectors change sign in the mirror plane. If the molecule in question posseses such a mirror symmetry, $\vec{D}$ and $\vec{C}$ vanish in the plane, as illustrated in Figure 1A.

The physics of the vectors are different, as shown in Figure 1B. The vector $\vec{C}$ is the vector around which the spin passing through the molecule precesses. The precession of a spin around an external field, $\vec{B}$ is precisely proportional to $\vec{B} \times \vec{a}$ to first order in the Zeeman

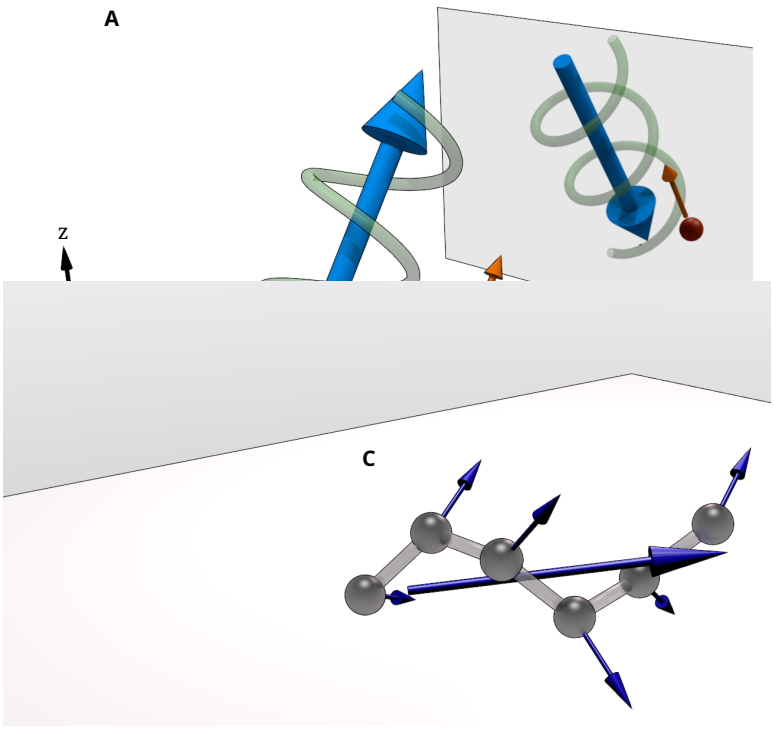

Figure 1: (**A**) Illustration of how the components of an axial vector, $\vec{D}$, and a polar vector, such as the velocity of an electron, $\vec{v}$, transforms under a mirror operation in the xz-plane. (**B**) Geometrical interpretation of how the vectors, $\vec{D}$ (blue) and $\vec{C}$ (green), affect the spin polarization of an electron current (purple). The $\vec{D}$-vector stretches the polarization along its axis, while the $\vec{C}$-vector rotates the spin about its axis. The final emerging polarization is a sum of the two effects. (**C**) Illustration of how the vectors result from sums of contributions located at each site of a molecule.

coupling.

The other vector, $\vec{D}$, is the most important in explaining the CISS effect, since a non-polarized electron will be polarized along $\vec{D}$ after emerging from the molecule. The key to understand and calculate the CISS effect is thus to consider the $\vec{D}$-vector.

Note that both vectors are given by a sum of contributions from each site. This is illustrated in Figure 1C. The direction of the vectors at each site depends on the details of the molecule and its coupling to the leads, as well as the energy of the incoming electron. However, in the idealized case of a molecule with helical symmetry, the local contributions from two adjacent sites are simply rotated by an angle around the helicity axis. Consequently, the contributions along the axis will add up. On the other hand, in the plane orthogonal to

the axis they cancel.

First, we will prove a general theorem about the $\vec{D}$-vector (see SI for details). Let us consider a situation where the probability p_i is only a function of the energy E_i. I.e. we assume that all states of the left lead with a given energy have the *same probability*. This would be the case if p_i represent a thermal distribution. In this case, $\gamma_L = n_F(E-\mu)\Gamma_L$ and a combination of Onsager's reciprocal relations and current conservation leads to

$$\vec{D} = 0. \tag{8}$$

We have assumed that there are no initial electrons in the right lead which could contribute to a current from right to left. This is actually a correct assumption for most CISS experiments, where the initial electron is created by a photo-excitation process in the left lead. This process is illustrated in Figure 2. Standard NEGF theory usually assumes that both left and right leads are metallic, and the current is induced by applying a voltage difference between the leads. The theorem *also* holds in that case.

This dramatic result explains many of the unpublished works where people base their calculations on some version of NEGF, with two leads consisting of Fermi seas of electrons. The polarizations found in these calculations are always in the per mille range, i.e. much smaller than the observed polarizations. Given the theorem above, we can understand that any polarization in systems of this kind must be of second order in the spin orbit coupling, and hence very small indeed.

Luckily, the theorem suggest a way out of this impasse. Actual experiments do not involve simple leads, where all states with a given energy contribute equally to the initial density matrix. Instead, certain initial states in the density matrix are more probable than others, e.g due to peculiarities of the initialization process. In the case of carriers created by photon absorption, selection rules of the absorption matrix element can break this "democracy" among initial states. The consequence is that γ_L is not proportional to Γ_L. Also, if there

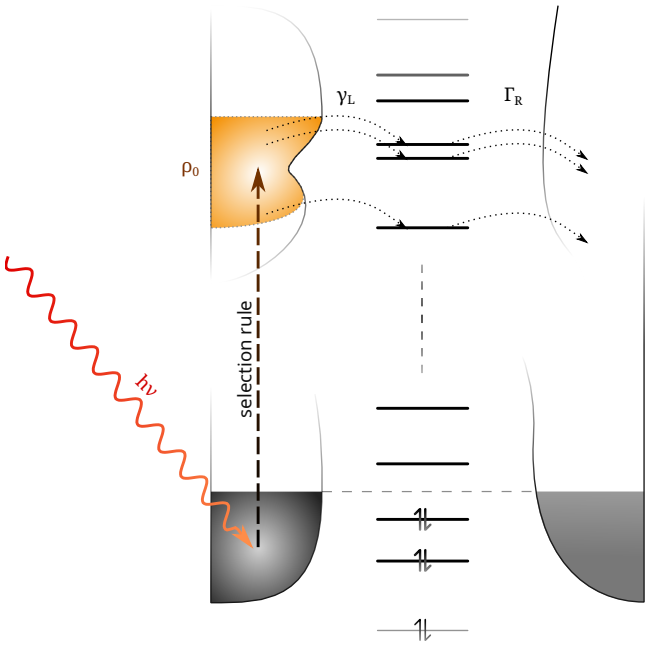

Figure 2: Schematic of the photo-excitation process. Electrons are excited by some selection rule into an unoccupied band. Because of the selection rule, not all excited states with the same energy are occupied with equal probability. As a result, electrons with one spin are favored over the other during transmission to the other side.

are more than two leads, then there will be a CISS effect to lowest order in the SO-coupling, as pointed out by Matityahu et al.[27] Note also that the $\vec{D}$-vector will reverse its direction, if we reverse the current, i.e. if the electron originates in the right lead.

Finally, in the experiment by Göhler et al.,[2] the spin polarization of the photo-excited electrons was measured using both linearly- and circularly polarized light. Depending on the polarization, different excitations and thus initial density matrices are generated. In the supplementary material, the interaction between the light and the electrons is analyzed for the different kinds of polarization: linear, clockwise and counter-clockwise. The result of this analysis is that the associated $\vec{D}$-vectors are related through:

$$\vec{D}_{\mathrm{cw}} = \vec{D}_{\mathrm{lin}} + \frac{1}{2}\Delta\vec{D}, \quad \vec{D}_{\mathrm{ccw}} = \vec{D}_{\mathrm{lin}} - \frac{1}{2}\Delta\vec{D}, \tag{9}$$

where $\Delta\vec{D}$ is conversely defined as $\Delta\vec{D} \equiv \vec{D}_{\mathrm{cw}} - \vec{D}_{\mathrm{ccw}}$. A similar equation holds for the

$\vec{C}$-vectors. Using Eq. (6), the $\vec{D}$-vector can be extracted from the equation

$$\vec{D} = \frac{1 - \vec{a}_{\rm in} \cdot \vec{a}_{\rm in}}{1 - \vec{a}_{\rm in} \cdot \vec{a}_{\rm out}} \vec{a}_{\rm out} - \vec{a}_{\rm in} - \vec{C} \times \vec{a}_{\rm in}, \quad |\vec{a}_{\rm in}| < 1. \tag{10}$$

Note that $\vec{C}$ is generally parallel to the molecule axis and, by assumption, so is $\vec{a}_{\rm in}$. Thus, the cross product vanishes. Plugging the experimental values for $\vec{a}_{\rm in}$, $\vec{a}_{\rm out}$ into Eq. (10), we indeed find that Eq. (9) is consistent with the experiment. This is summarized in Table 1.

Table 1: Comparison of the magnitude of the extracted $\vec{D}$-vectors from the experiment by Göhler et al.[2]

Length	$D_{\rm cw}$ (%)	$D_{\rm ccw}$ (%)	$(D_{\rm cw} + D_{\rm ccw})/2$ (%)	$D_{\rm lin}$ (%)
50-bp	−48	−14	−31	−31
78-bp	−68	−45	−57	−57

Magnetic leads

In another class of experiments, the CISS effect is inferred from an experiment, where the right lead is magnetized along a certain direction, $\vec{m}$. The current is generated by applying a bias voltage across the leads which are otherwise in thermal equilibrium. The current in the device is measured to have a value, I_+. Next, the magnetization of the lead is reversed, and the current is measured to have the value, I_-. A difference between the two currents is taken as evidence of the CISS effect.

This setup differs in subtle ways from the photo-excitation experiments, and requires careful analysis. The general theory of a current passing between metallic leads through a molecule has been widely studied. The formula for the current into the right lead, reviewed in the supplementary material, says that:

$$I_+ = \int \big(T_{LR}(\vec{m}) n_F(E - \mu_L) - T_{RL}(\vec{m}) n_F(E - \mu_R) \big) \frac{dE}{2\pi}. \tag{11}$$

The transmission functions satisfy the Onsager relation $T_{RL}(\vec{m}) = T_{LR}(-\vec{m})$. Without SO-

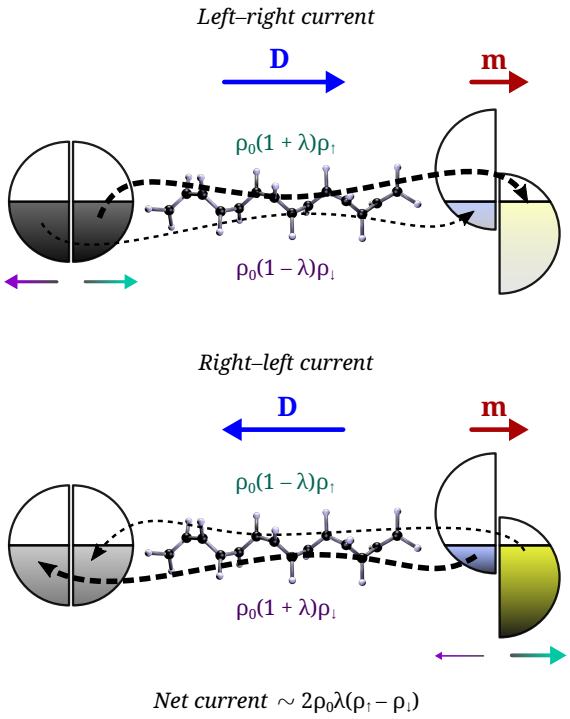

Figure 3: Schematic illustration of a net current when having one magnetized lead and a chiral molecule with SO-coupling. The $\vec{D}$-vector associated with the chiral molecule is assumed to be parallel with the magnetization. ρ_0 is a measure of the density of states in the left lead. The parameter λ describes the enhanced transmission of electrons with spin along the $\vec{D}$-vector. $\rho_\uparrow$ and $\rho_\downarrow$ are measures of the density of states of electrons in the right lead with spins parallel and antiparallel to $\vec{m}$, respectively.

coupling, $T_{LR}(\vec{m})$ is an even function of $\vec{m}$, but with SO-coupling, the transmission will have a contribution which is linear in $\vec{m}$ and the SO-coupling:

$$T_{LR}(\vec{m}) = T^0_{LR}\left(1 + \vec{D}\cdot\vec{m}\right). \tag{12}$$

Here the $\vec{D}$-vector is again characteristic of a chiral molecule with SO-coupling, and theoretically given by a formula equivalent to the one described in the previous section. In this context, the consequence of such a term is profound. Consider the current *without bias*. In that case, $\mu_L = \mu_R = \mu$ and the current becomes

$$I^0_+ = 2\int T^0_{LR}\,\vec{D}\cdot\vec{m}\,n_F(E-\mu)\frac{dE}{2\pi}. \tag{13}$$

In general, this integral will be non-zero and thus our initial, unpolarized density matrix of the left lead cannot be the correct one in physical equilibrium. In Figure 3, we show how such a current arises based on simple considerations. We can learn what is going on by calculating the spin current in this "false" equilibrium. Since spin is a vector quantity, and we have two other vectors in the problem—the magnetization $\vec{m}$ and angular momentum $\vec{\Lambda}$—we expect a spin current into the left lead given by

$$\frac{d}{dt}\langle\vec{\sigma}\rangle_L = \int T^0_{RL}\left(\vec{D}_1\times\vec{m} + (\vec{D}_2\cdot\vec{m})\vec{m}\right) n_F(E-\mu)\frac{dE}{2\pi}, \tag{14}$$

where both $\vec{D}_1$ and $\vec{D}_2$ are linear in the SO-coupling. Eq. (14) tells us that spin is being transported to the left lead. This process will gradually build up a magnetization in the left lead close to the chiral molecule. The process will stop at some point and a new equilibrium situation with no currents will be established. The difference is that the left lead will be magnetized locally, with a magnetization $\vec{a}_+$ which is related to $\vec{m}$. According to Eq. (14), we expect that $\vec{a}_+$ has components perpendicular and parallel to $\vec{m}$. Note, however, that the former term changes sign if $\vec{m}$ is reversed, while the latter is unchanged.

We can now redo the current calculation using the new equilibrium state. We get:

$$I_+ = \int T^0_{LR}\,(1 + A\,\vec{m}\cdot\vec{a}_+)\,(n_F(E-\mu_L) - n_F(E-\mu_R))\,\frac{dE}{2\pi}. \tag{15}$$

This time, there is no equilibrium current. The function A is given by:

$$A = \frac{\mathrm{Tr}[\Delta\Gamma_L G^\dagger_M \Delta\Gamma_R G_M]}{\mathrm{Tr}[\Gamma_L G^\dagger_M \Gamma_R G_M]},$$

where $\Delta\Gamma_L$, $\Delta\Gamma_R$ are the difference in coupling to the leads for spins parallel and anti-parallel to the magnetization of the left and right lead, respectively.

If the magnetization is reversed, the induced local magnetization in the left lead is changed

to $\vec{a}_-$. The difference between the currents of opposite magnetizations is now given by

$$I_+ - I_- = \int T^0_{LR} A \, \vec{m} \cdot (\vec{a}_+ + \vec{a}_-) \left(n_F(E - \mu_L) - n_F(E - \mu_R) \right) \frac{dE}{2\pi}, \tag{16}$$

and since $\vec{a}_+ \neq -\vec{a}_-$, this will be finite even at low bias. The expression does not involve the SO-coupling directly. Indirectly, though, the presence of the chiral molecules with their SO-coupling helps establish a new ground state with finite magnetization of both leads, and this is the ground state being perturbed by a bias.

Calculations

To illustrate the points made in the theory outlined above, we will consider a family of carbohydrate molecules. They do not necessarily exist in nature by themselves, but similar chains of atoms can be found in backbones of more realistic chiral molecules. The theoretical molecule is twisted polyacetylene, illustrated in Figure 4A. The carbon atoms in the chain form a helix with fixed radius, where each atom is placed an angle φ apart. The pitch of the helix is held fixed, so that the geometry only has one parameter, φ.

An extra hydrogen atom has been attached to the carbon atoms at both ends. In the limits $\varphi = 0$ and $\varphi = \pi$ the resulting molecules become achiral.

We have implemented the perturbation theory described in the sections above using a tight-binding model for this molecule. The implementation uses a generic set of Slater-Koster hopping parameters,[36] and the code can be found in the supporting material. The results of the implementation are summarized in Figure 4B-D. Importantly, we are considering coupling matrices γ_L, which are *not* proportional to Γ_L. We note that $\vec{D}$ only gets a sizeable value near level crossings (degeneracies). This is to be expected in perturbation theory, since only in places where energy gaps are of the same order of magnitude as the perturbation will the perturbation have a chance of getting large. The molecule is perturbed by two effects: coupling to the leads, and the SO-coupling. The former coupling is treated in an

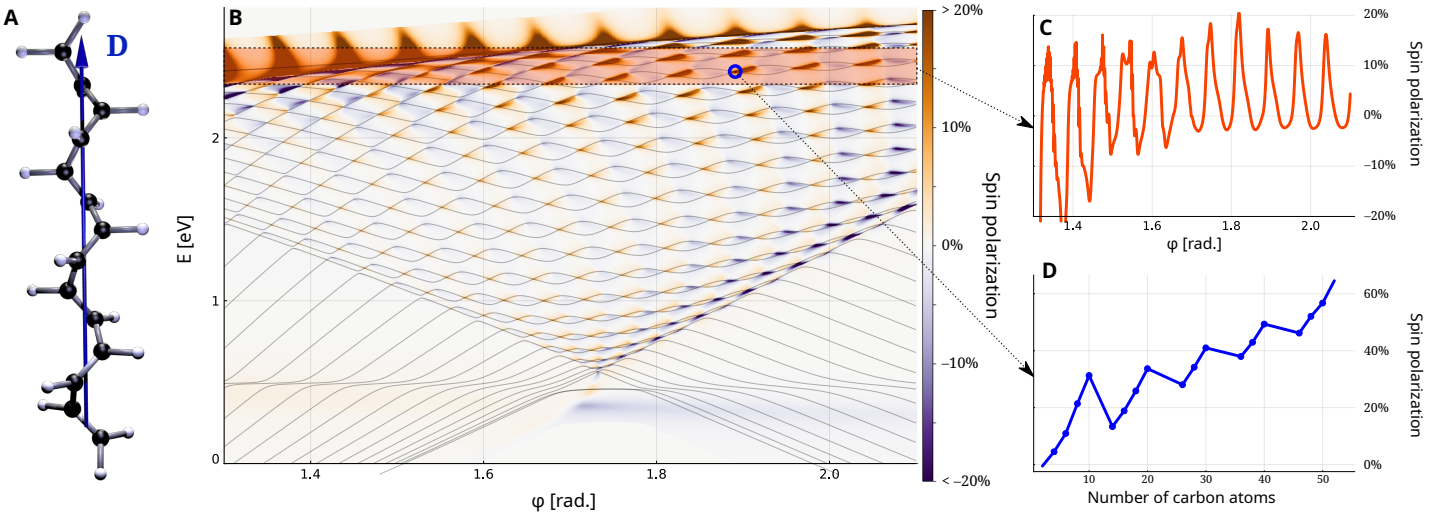

Figure 4: (**A**) Illustration of the helical polyacetylene molecule with a length of 14 carbon atoms and $\varphi \sim \pi/2$. The blue arrow indicates the direction along which the $\vec{D}$-vector generally points near level crossings. (**B**) Molecular energy levels (black lines) for a molecule with a length of 38 carbon atoms as a function of φ. The color shows the spin polarization for an electron with energy E. The integral of the polarization weighted by the transmission, over the energy window indicated by the orange box, is shown in (**C**). The resulting polarization is dominated by energies with higher transmission. In photo-excitation experiments, the excited electrons will have a wide energy distribution, and thus this observation is key to the understanding of these experiments. (**D**) Shows the length dependence of the peak of the polarization for the crossing marked by the blue circle. For different lengths, the exact energy and geometry at which a crossing is found varies, which is reflected in the jagged shape of the curve.

exact manner in the theory, while the latter is treated to first order. At level crossings in the unperturbed molecule, say when states $|1\rangle$ and $|2\rangle$ are degenerate, we can calculate $\vec{D}$ explicitly.

It is important to note the fact that the angular momentum operator $\vec{\Lambda}$ only has off-diagonal matrix elements. This follows from the fact that $\vec{\Lambda}$ is purely imaginary and Hermitian, and the states $|1\rangle$ and $|2\rangle$ are purely real. Consequently, the matrix elements are antisymmetric: $\vec{\Lambda}_{12} = -\vec{\Lambda}_{21}$. With this observation we get that the $\vec{D}$-vector at a crossing is given by

$$\vec{D} = (i\vec{\Lambda}_{12}) f_{12}, \quad \text{where,} \quad f_{12} = \frac{\langle 1|\Gamma^{-1}\left(\Gamma_R\Gamma^{-1}\gamma_L - \gamma_L\Gamma^{-1}\Gamma_R\right)\Gamma^{-1}|2\rangle}{\mathrm{Tr}[\gamma_L\Gamma^{-1}\Gamma_R\Gamma^{-1}]}. \tag{17}$$

This is an interesting formula in many respects. First of all, it shows that spin polarization is controlled by the angular momentum transition matrix element $i\vec{\Lambda}_{12}$, which controls spin-flip processes. It is reminiscent of the dipole matrix element which controls the absorption and emission of photons. It is also clear that in the case where γ_L is proportional to $\Gamma - \Gamma_R$, the polarization vanishes, as predicted by the general theory. For the crossing indicated by a blue circle in Figure 4B, the matrix elements are $i\Lambda^z_{12} = 0.62$ meV and $f_{12} = 0.69$ meV^{-1}.

From Eq. (17), we can also make a statement about how the spin polarization scales with the length of the molecule. Assume that the molecule contains N atoms. Then, the part of the wave function of a molecular orbital residing on a single atom scales as $1/\sqrt{N}$. Since the couplings to the outside leads are local to the ends of the molecule, we expect elements of the Γ matrices to scale as $1/N$. $\vec{\Lambda}$, on the other hand, is a sum of N atomic terms, and thus $i\vec{\Lambda}_{12}$ does not scale with N. With these observations, we expect a scaling of $\vec{D} \sim N$, which is indeed the case, as shown in Figure 4D. Such a scaling is also observed in experiments on DNA molecules.[2]

Conclusion

There are at least two general and robust reasons why the CISS effect is surprising from a theoretical point of view. First, the spin-orbit coupling is around 6 meV for carbon atoms. Compared to typical molecular and thermal energy scales, this is very small. Second, although a single electron passing through a chiral molecule can be polarized, the average polarization for all electrons tend to cancel. Indeed, we have proven in this paper, that if all electrons with a given energy in the incoming lead are equally probable, the average polarization is zero to leading order in the SO-coupling. We have shown how to overcome this conundrum. First, if there are degeneracies in the molecular spectrum, the SO-coupling does not have to be a small perturbation and the polarization can become large. The polarization will depend on the coupling to the in- and outgoing leads, which is now the relevant energy

to compare with. Next, in one class of experiments the in-electrons are generated optically by a laser. Thus, given selection rules in the photon absorption process, states with same energy can have very different probabilities.

In a second class of experiments, where the presence of a magnetic lead is essential, a new theoretical challenge emerges. In the naive equilibrium state with two thermal leads—one being magnetic—and a chiral molecule with SO-coupling, one finds a spin-polarized current. This means that in the correct equilibrium state, both leads are magnetically polarized. Thus, changing the magnetic field does more than just reverse the spin of the carriers.

Detailed calculations still need to be performed on concrete systems. However, the points made in this paper should be the basis of a correct analysis. The methodology, based on a perturbative approach to the spin-orbit interaction, is general, and can be implemented in numerical calculations based on NEGF and DFT.

Acknowledgments

We thank Ron Naamann and other participants at Telluride workshop on CISS for very fruitful discussions.

Supplementary materials

All mathematical and modelling details can be found in a supplementary manuscript.

References

(1) Ray, K.; Ananthavel, S. P.; Waldeck, D. H.; Naaman, R. Asymmetric Scattering of Polarized Electrons by Organized Organic Films of Chiral Molecules. *Science* **1999**, *283*, 814–816.

(2) GÃűhler, B.; Hamelbeck, V.; Markus, T. Z.; Kettner, M.; Hanne, G. F.; Vager, Z.; Naaman, R.; Zacharias, H. Spin Selectivity in Electron Transmission Through Self-Assembled Monolayers of Double-Stranded DNA. *Science* **2011**, *331*, 894.

(3) Xie, Z.; Markus, T. Z.; Cohen, S. R.; Vager, Z.; Gutierrez, R.; Naaman, R. Spin Specific Electron Conduction through DNA Oligomers. *Nano Lett.* **2011**, *11*, 4652–4655.

(4) Ben Dor, O.; Morali, N.; Yochelis, S.; Baczewski, L. T.; Paltiel, Y. Local Light-Induced Magnetization Using Nanodots and Chiral Molecules. *Nano Lett.* **2014**, *14*, 6042–6049.

(5) Kiran, V.; Mathew, S. P.; Cohen, S. R.; HernÃąndez Delgado, I.; Lacour, J.; Naaman, R. HelicenesâĂŤA New Class of Organic Spin Filter. *Adv. Mater.* **2016**, *28*, 1957–1962.

(6) Eckshtain-Levi, M.; Capua, E.; Refaely-Abramson, S.; Sarkar, S.; Gavrilov, Y.; Mathew, S. P.; Paltiel, Y.; Levy, Y.; Kronik, L.; Naaman, R. Cold denaturation induces inversion of dipole and spin transfer in chiral peptide monolayers. *Nature Communications* **2016**, *7*, 10744.

(7) Mondal, P. C.; Roy, P.; Kim, D.; Fullerton, E. E.; Cohen, H.; Naaman, R. Photospintronics: Magnetic Field-Controlled Photoemission and Light-Controlled Spin Transport in Hybrid Chiral Oligopeptide-Nanoparticle Structures. *Nano Lett.* **2016**, *16*, 2806–2811.

(8) Alpern, H.; Katzir, E.; Yochelis, S.; Katz, N.; Paltiel, Y.; Millo, O. Unconventional

superconductivity induced in Nb films by adsorbed chiral molecules. *New J. Phys.* **2016**, *18*, 113048.

(9) Alam, K. M.; Pramanik, S. Spin filtering with poly-T wrapped single wall carbon nanotubes. *Nanoscale* **2017**, *9*, 5155–5163.

(10) Abendroth, J. M.; Nakatsuka, N.; Ye, M.; Kim, D.; Fullerton, E. E.; Andrews, A. M.; Weiss, P. S. Analyzing Spin Selectivity in DNA-Mediated Charge Transfer via Fluorescence Microscopy. *ACS Nano* **2017**, *11*, 7516–7526.

(11) Kumar, A.; Capua, E.; Kesharwani, M. K.; Martin, J. M. L.; Sitbon, E.; Waldeck, D. H.; Naaman, R. Chirality-induced spin polarization places symmetry constraints on biomolecular interactions. *PNAS* **2017**, *114*, 2474–2478.

(12) AragonÃĺs, A. C.; Medina, E.; FerrerâĂŘHuerta, M.; Gimeno, N.; TeixidÃş, M.; Palma, J. L.; Tao, N.; Ugalde, J. M.; Giralt, E.; DÃŋezâĂŘPÃĭrez, I.; Mujica, V. Measuring the Spin-Polarization Power of a Single Chiral Molecule. *Small* **2017**, *13*, 1602519.

(13) Varade, V.; Markus, T.; Vankayala, K.; Friedman, N.; Sheves, M.; Waldeck, D. H.; Naaman, R. Bacteriorhodopsin based non-magnetic spin filters for biomolecular spintronics. *Phys. Chem. Chem. Phys.* **2018**, *20*, 1091–1097.

(14) Santos, J. I.; Rivilla, I.; CossÃŋo, F. P.; Matxain, J. M.; Grzelczak, M.; Mazinani, S. K. S.; Ugalde, J. M.; Mujica, V. Chirality-Induced Electron Spin Polarization and Enantiospecific Response in Solid-State Cross-Polarization Nuclear Magnetic Resonance. *ACS Nano* **2018**, *12*, 11426–11433.

(15) Gazzotti, M.; Arnaboldi, S.; Grecchi, S.; Giovanardi, R.; Cannio, M.; Pasquali, L.; Giacomino, A.; Abollino, O.; Fontanesi, C. Spin-dependent electrochemistry: Enantioselectivity driven by chiral-induced spin selectivity effect. *Electrochimica Acta* **2018**, *286*, 271–278.

(16) Shapira, T.; Alpern, H.; Yochelis, S.; Lee, T.-K.; Kaun, C.-C.; Paltiel, Y.; Koren, G.; Millo, O. Unconventional order parameter induced by helical chiral molecules adsorbed on a metal proximity coupled to a superconductor. *Phys. Rev. B* **2018**, *98*, 214513.

(17) Ghosh, K. B.; Zhang, W.; Tassinari, F.; Mastai, Y.; Lidor-Shalev, O.; Naaman, R.; MÃűllers, P.; NÃijrenberg, D.; Zacharias, H.; Wei, J.; Wierzbinski, E.; Waldeck, D. H. Controlling Chemical Selectivity in Electrocatalysis with Chiral CuO-Coated Electrodes. *J. Phys. Chem. C* **2019**, *123*, 3024–3031.

(18) Yeganeh, S.; Ratner, M. A.; Medina, E.; Mujica, V. Chiral electron transport: Scattering through helical potentials. *J. Chem. Phys.* **2009**, *131*, 014707.

(19) Guo, A.-M.; Sun, Q.-f. Spin-Selective Transport of Electrons in DNA Double Helix. *Phys. Rev. Lett.* **2012**, *108*, 218102.

(20) Gutierrez, R.; DÃŋaz, E.; Naaman, R.; Cuniberti, G. Spin-selective transport through helical molecular systems. *Phys. Rev. B* **2012**, *85*, 081404.

(21) Gutierrez, R.; DÃŋaz, E.; Gaul, C.; Brumme, T.; DomÃŋnguez-Adame, F.; Cuniberti, G. Modeling Spin Transport in Helical Fields: Derivation of an Effective Low-Dimensional Hamiltonian. *J. Phys. Chem. C* **2013**, *117*, 22276–22284.

(22) Guo, A.-M.; DÃŋaz, E.; Gaul, C.; Gutierrez, R.; DomÃŋnguez-Adame, F.; Cuniberti, G.; Sun, Q.-f. Contact effects in spin transport along double-helical molecules. *Phys. Rev. B* **2014**, *89*, 205434.

(23) Guo, A.-M.; Sun, Q.-F. Spin-dependent electron transport in protein-like single-helical molecules. *PNAS* **2014**, *111*, 11658–11662.

(24) Wu, H.-N.; Zhu, Y.-L.; Sun, X.; Gong, W.-J. Spin polarization and spin separation realized in the double-helical molecules. *Physica E: Low-dimensional Systems and Nanostructures* **2015**, *74*, 156–159.

(25) Medina, E.; GonzÃąlez-Arraga, L. A.; Finkelstein-Shapiro, D.; Berche, B.; Mujica, V. Continuum model for chiral induced spin selectivity in helical molecules. *J. Chem. Phys.* **2015**, *142*, 194308.

(26) Michaeli, K.; Naaman, R. Origin of spin dependent tunneling through chiral molecules. *arXiv:1512.03435 [cond-mat]* **2015**, arXiv: 1512.03435.

(27) Matityahu, S.; Utsumi, Y.; Aharony, A.; Entin-Wohlman, O.; Balseiro, C. A. Spin-dependent transport through a chiral molecule in the presence of spin-orbit interaction and nonunitary effects. *Phys. Rev. B* **2016**, *93*, 075407.

(28) Varela, S.; Mujica, V.; Medina, E. Effective spin-orbit couplings in an analytical tight-binding model of DNA: Spin filtering and chiral spin transport. *Phys. Rev. B* **2016**, *93*, 155436.

(29) Pan, T.-R.; Guo, A.-M.; Sun, Q.-F. Spin-polarized electron transport through helicene molecular junctions. *Phys. Rev. B* **2016**, *94*, 235448.

(30) Matityahu, S.; Aharony, A.; Entin-Wohlman, O.; Balseiro, C. A. Spin filtering in all-electrical three-terminal interferometers. *Phys. Rev. B* **2017**, *95*, 085411.

(31) DÃŋaz, E.; Contreras, A.; HernÃąndez, J.; DomÃŋnguez-Adame, F. Effective nonlinear model for electron transport in deformable helical molecules. *Phys. Rev. E* **2018**, *98*, 052221.

(32) DÃŋaz, E.; DomÃŋnguez-Adame, F.; Gutierrez, R.; Cuniberti, G.; Mujica, V. Thermal Decoherence and Disorder Effects on Chiral-Induced Spin Selectivity. *J. Phys. Chem. Lett.* **2018**, *9*, 5753–5758.

(33) Maslyuk, V. V.; Gutierrez, R.; Dianat, A.; Mujica, V.; Cuniberti, G. Enhanced Magnetoresistance in Chiral Molecular Junctions. *J. Phys. Chem. Lett.* **2018**, *9*, 5453–5459.

(34) NÃijrenberg, D.; Zacharias, H. Evaluation of spin-flip scattering in chirality-induced spin selectivity using the Riccati equation. *Phys. Chem. Chem. Phys.* **2019**, *21*, 3761–3770.

(35) Yang, X.; van der Wal, C. H.; van Wees, B. J. Spin-dependent electron transmission model for chiral molecules in mesoscopic devices. *Phys. Rev. B* **2019**, *99*, 024418.

(36) Elstner, M.; Porezag, D.; Jungnickel, G.; Elsner, J.; Haugk, M.; Frauenheim, T.; Suhai, S.; Seifert, G. Self-consistent-charge density-functional tight-binding method for simulations of complex materials properties. *Phys. Rev. B* **1998**, *58*, 7260–7268.